Journal of Biomedical Optics 8(4), 636–641 (October 2003)

Optical imaging of metastatic tumors using a folate-targeted fluorescent probe

Michael D. Kennedy
Karim N. Jallad
David H. Thompson
Dor Ben-Amotz
Philip S. Low
Purdue University
Department of Chemistry
West Lafayette, Indiana 47907
E-mail: plow@purdue.edu

Abstract. We describe the use of a tumor targeting ligand, the vitamin folic acid, to deliver an attached fluorescent probe to both primary and metastatic tumors overexpressing the folate receptor. Upon laser excitation, derived images of normal tissues generally show little or no fluorescence, whereas images of folate receptor-expressing tumors display bright fluorescence that can be easily distinguished from adjacent normal tissue. Furthermore, metastatic tumor loci of submillimeter size can also be visualized without the aid of image processing or enhancement. The sharp distinction between tumor and normal tissues provided by this technique could find application in the localization and resection of tumor tissue during surgery or in the enhanced endoscopic detection and staging of cancers. *© 2003 Society of Photo-Optical Instrumentation Engineers.* [DOI: 10.1117/1.1609453]

Keywords: folate receptor; optical imaging of tumors; tumor targeting; folate-fluorescent probe conjugates.

Paper 02089 received Dec. 11, 2002; revised manuscript received Apr. 30, 2003; accepted for publication May 7, 2003.

1 Introduction

In vivo tumor imaging requires the establishment of contrast between the tumor and surrounding normal tissues. Magnetic resonance imaging (MRI) techniques rely on differences in water relaxivity between malignant lesions and healthy cells to achieve contrast. Positron emission tomography (PET) imaging methodologies generally exploit differences in metabolic rates between cancer and normal cells to allow visualization of tumors. Some radiological imaging methods rely on the elevated passive vascular permeability of many neoplasms to achieve contrast with healthy tissues.[1] Finally, a few imaging protocols exploit the overexpression of certain receptors on cancer cells to target attached imaging or contrast agents specifically to malignant cells. Examples of targeting ligands exploited for the delivery of imaging agents include antibodies,[2] hormones,[3] small peptides,[4,5] and the vitamin folic acid.[6]

Folic acid-based targeting strategies rely on (1) the high affinity of folate for its cell surface receptor ($K_d \sim 10^{-10}$) (Ref. 7), (2) the absence or inaccessibility of the receptor on normal cells [the folate receptor (FR) on those normal cells that express it is primarily confined to the apical surface of polarized epithelia where it is not easily accessed from the blood],[8] and (3) the elevated expression of the receptor on many tumor cells. Those tumors that commonly overexpress FR include cancers of the ovary,[9] breast,[10] kidney,[11] lung,[10,12] endometrium,[10] myeloid cells,[13] and brain.[8,14] Diagnostic imaging of folate receptor-expressing tumors using folate-conjugated gamma scintigraphy or MRI contrast agents generally yields good contrast with adjacent normal tissues.[15,16] Optical imaging of receptor-expressing tumors using folate-linked dyes has also recently been explored.[17,18]

While scintigraphic and MRI techniques often offer the sensitivity needed to detect metastatic lesions noninvasively, targetable fluorescent agents may find applications where use of the these methodologies is inadequate. Thus, during debulking surgery, where malignant loci can be difficult to identify, the presence of a fluorescent signal might assist the surgeon in locating them. Furthermore, when tumors are situated near the body surface and analysis of tumor progression is repeatedly required, optical imaging methodologies can often be applied without danger of toxicity. Also, in the course of an endoscopic examination,[19–21] fluorescence imaging can allow the precise assessment of the location, size, and invasiveness of a tumor. Finally, optical imaging instruments may be simpler and less expensive to operate than those required for other imaging technologies, permitting their eventual application by less specialized medical centers.

In this paper we demonstrate the ability to visualize folate receptor-expressing cancer tissues in various peritoneal, subcutaneous, and metastatic murine tumor models following intravenous administration of a folate-fluorescein conjugate. Because tumors as small as a few millimeters can be easily detected without image processing or enhancement, and since malignant lesions smaller than 0.5 mm can be located with appropriate optical instrumentation, these results provide an incentive for the development of folate-targeted fluorophores as aids in the localization and characterization of tumors during surgery and endoscopic examination.

2 Experimental

2.1 *Materials*

Amino fluorescein was purchased from Sigma-Aldrich (St. Louis, Missouri). Folate-fluorescein was kindly provided by Endocyte Inc. (West Lafayette, Indiana). The folate-fluorescein conjugate contains an ethylenediamine bridge linking the γ-carboxyl of folate via an amide bond on one end to the isothiocyanate group of fluorescein isothiocyanate on

1083-3668/2003/$15.00 © 2003 SPIE

the other end. The synthesis of γ-carboxyl-linked folate-fluorescein was described in a previous report.[22] Methotrexate-fluorescein was purchased from Molecular Probes (Eugene, Oregon).

2.2 *Cell Culture*

M109 cells, a murine lung carcinoma cell line of BALB/c mouse origin, were grown subcutaneously in BALB/c mice. In order to retain high viability in BALB/c mice, the M109 cells were discarded after the fourth passage in culture. L1210 cells, a lymphocyte-derived cell line of DBA mouse origin, were cultured in folate-free RPMI with a change of medium every three to four days.

2.3 *Animal Studies*

All animal procedures were carried out with approval from the Purdue animal care and use committee. BALB/c or DBA mice were placed on a folate-deficient diet (Dyets, Bethlehem, Pennsylvania) three weeks prior to each experiment to lower the folate levels in the blood to the physiological range.[23] Tumors were induced subcutaneously by injecting 100 μl of cell culture solution containing ~500,000 M109 or L1210 cells. Imaging of mice with subcutaneous tumors was performed when the tumors reached approximately 200 mm^3 in size. For intraperitoneal (i.p.) tumors, ~500,000 M109 or L1210 cells were implanted in the peritoneal cavity and allowed to proliferate for approximately two weeks prior to analysis, which is sufficient time for tumor masses >1 mm^3 to appear. Metastatic tumors were initiated by injection of ~200,000 M109 or L1210 cells into the femoral vein, and the imaging was performed two weeks afterward in a variety of tissues.

The folate-fluorescein conjugate, methotrexate-fluorescein, or the nontargeted control, fluorescein amine, was injected into the femoral vein of mice by making an incision in the leg to expose the vein. One hundred microliters of a phosphate-buffered saline (PBS) solution containing 10 nmol of folate-fluorescein conjugate or fluorescein amine was then injected and images were collected 2 h later. The amount of imaging agent injected and the waiting period between injection and imaging were both chosen based on preliminary studies aimed at optimizing fluorescence contrast (not shown). The wound was closed using Vetbond (Butler Co., Indianapolis, Indiana), and the mice were euthanized at the specified times prior to imaging.

2.4 *Laser Imaging and Spectral Analysis*

Whole-tissue fluorescent imaging was performed using an imaging system consisting of an argon laser (Spectra-Physics, Mountain View, California) operating at 488 nm with a total laser power of 200 mW reaching the 2-cm sample field of view. Fluorescence was detected by a colored CCD camera (JAI CV-S3200N) (Edmund Industrial Optics, Barrington, New Jersey) with a sensing area of 768×494 pixels and a pixel size of 8.4×9.8 μm^2. An f/5.6 152- to 457-mm 10× CCD zoom lens (Edmund Industrial Optics) was used to collect fluorescence from the 2.0×2.0-cm field of view. A bandpass filter with <80% T at 515 to 585 nm (Intor Inc., Socorro, New Mexico) was placed between the lens and the CCD in order to reject laser light and suppress tissue autofluorescence outside the fluorescein fluorescence band. The images were digitally acquired using Snappy software v. 4.0 (Play Inc., Sacramento, California).

Fluorescence spectra were obtained using a separate setup with a thermoelectric-cooled CCD (ST6, SBIG Instruments, Santa Barbara, California) with 375×242 pixels and a pixel size of 23×25 μm^2. In this case, the same laser was used to illuminate a 5-mm diameter of a sample placed on an Olympus BH-2 microscope stage (Olympus Inc., Melville, New York). The fluorescent light was collected with a 4× objective and directed from the sample toward a holographic Super-Notch filter (HNF, Kaiser Optical, Ann Arbor, Michigan) using a 99% reflective mirror placed above the microscope objective. The HNF is used to reject the laser light at 488 nm, and the fluorescent light transmitted through the HNF is focused on the spectrograph (Spectra Pro-150, Acton Research Corp., Acton, Massachusetts) entrance (slit width=200 μm) using a lens of 21 mm focal length. The spectrograph is equipped with a 600-g/mm grating tuned to a wavelength of 535 nm and spanning a 495- to 575-nm window on the CCD detector. The fluorescence spectra were acquired using Kestrel Spec software (Princeton Instruments, Trenton, New Jersey) with an integration time of 5 s, and fluorescence wavelengths were calibrated against neon lamp calibration lines. Spectra were taken of various tissues removed from three mice 2 h after an injection with 10 nmol of folate-linked fluorescein. Spectra were also taken of control samples taken from three mice with nothing injected.

3 Results

BALB/c and DBA mice were implanted subcutaneously with M109 and L1210 cultured cancer cells, respectively, and tumors were allowed to grow to ~200 mm^3. Two hours following intravenous injection of folate-fluorescein, the tumor-bearing mice were euthanized and their tumors imaged using both normal light and laser (fluorescence view) illumination. As seen in Fig. 1, tumor masses were significantly more fluorescent than adjacent normal tissues. In fact, the differences in fluorescence intensity were readily apparent without background subtraction or other image-processing methods used in previous reports.[24,25] The absence of tumor fluorescence upon coinjection of excess free folate [Figs. 1(c) and 1(d)] further shows that the tumor uptake is completely folate mediated. No significant loss of fluorescence could be visually detected during the time used for imaging, even after 1 h of illumination by the laser (data not shown). Although some areas of the tumor tissue showed minor variations in fluorescence intensity, all tumor areas fluoresced brightly, as shown by the spectral analysis described later. Other studies have also shown that folate receptor expression is uniform throughout the tumor (unpublished observations). These data suggest that folate-linked fluorophores might be useful for optical imaging wherever tumor location allows access to incident and fluorescent light.

To more accurately quantitate the difference in the targeted fluorescence between normal and malignant tissues, it was decided to examine the spectral properties of various tissues using more analytical spectrofluorimetric methods. For this purpose, tissue samples from both folate-fluorescein injected

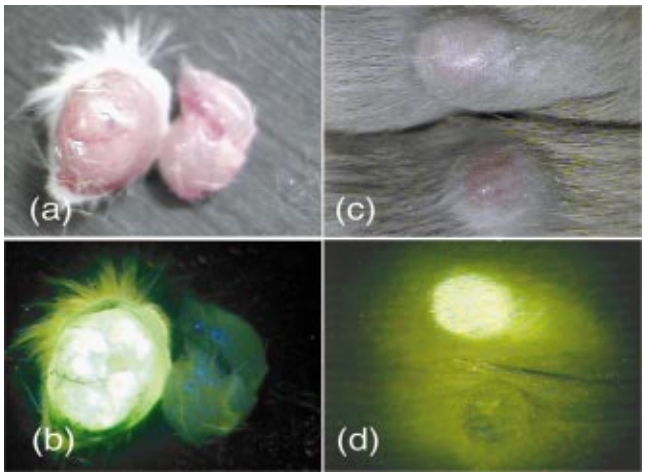

Fig. 1 Targeting of folate-fluorescein to L1210 subcutaneous tumors. Mice were injected intravenously (femoral vein) with 10 nmol of folate-fluorescein and sacrificed 2 h later. Another mouse was coinjected with a 100-fold molar excess of folic acid. Panels (a) and (b) display M109 subcutaneous tumors (left tissue sample) next to muscle (right) tissue isolated from the same mouse. Panel (c) shows the white light image and panel (d) shows the fluorescent image of L1210 subcutaneous tumors from a mouse injected with folate-fluorescein (top tumor) or folate-fluorescein plus 100-fold molar excess of free folate (bottom tumor).

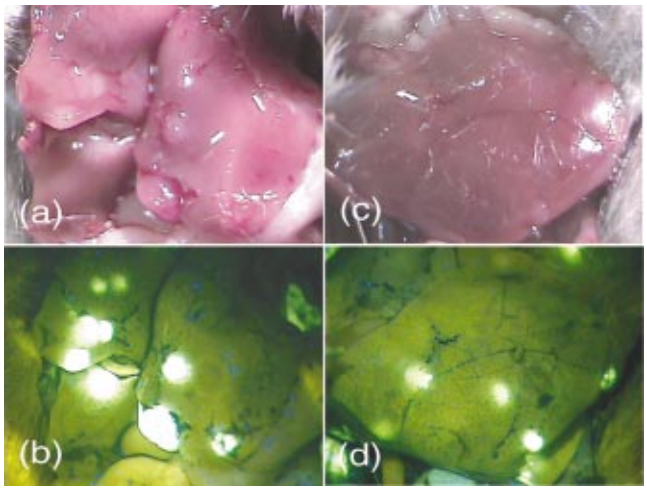

Fig. 4 Images of L1210 metastatic tumor nodules in the liver of a DBA mouse. The mouse was injected intravenously (femoral vein) with 10 nmol of folate-fluorescein and imaged 2 h later. Panels (a) and (b) show the white light and fluorescent light images of the lower lobe of the liver, while panels (c) and (d) display the same images of the upper lobe of the liver.

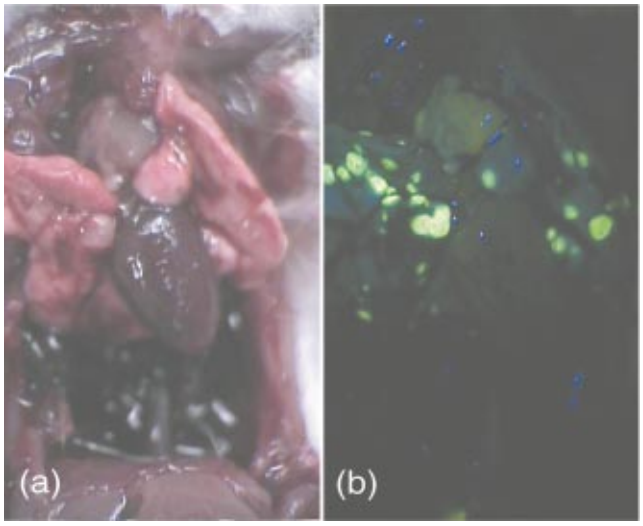

Fig. 3 Optical images of multiple metastatic M109 tumor nodules in a mouse lung 2 h after intravenous (femoral vein) injection of 10 nmol of folate-fluorescein. (a) Normal light image of the opened chest cavity. (b) Same chest cavity visualized under 488-nm argon laser illumination.

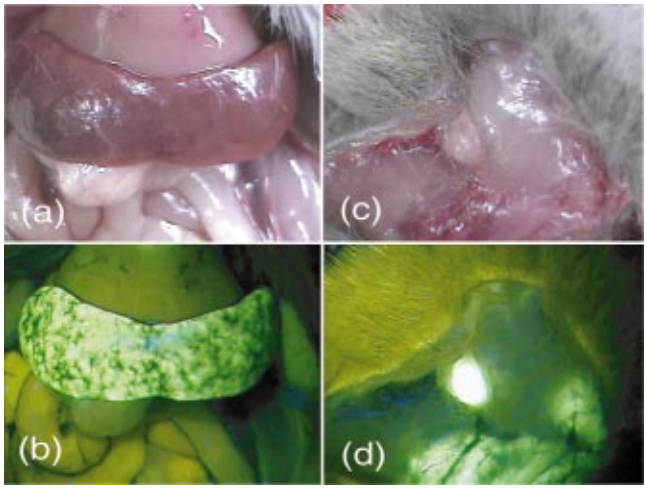

Fig. 5 L1210 tumor nodules in the spleen and muscle tissue of a DBA mouse are detectable after injection of folate-fluorescein. The mice were treated as in Fig. 4. Panels (a) and (b) show the white light and fluorescent light images of a tumor-infiltrated spleen, and panels (c) and (d) display the same images of a tumor nodule in the skeletal muscle of the neck.

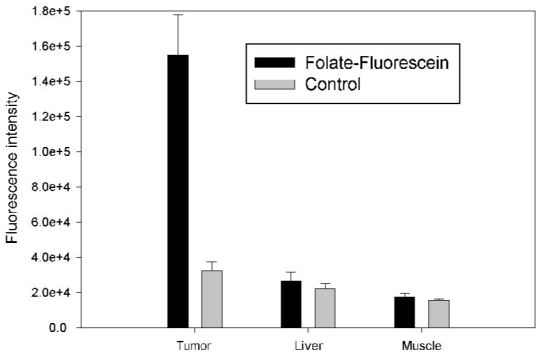

Fig. 2 Comparison of the fluorescence intensity of tissues from mice injected with folate-fluorescein or buffer control. Tissues were dissected 2 h after folate-fluorescein or buffer injection and spectra of both groups were measured as described in Sec. 2.4. The data points represent the average intensities of the indicated tissues from three mice.

and noninjected tumor-bearing mice were examined using a spectrograph equipped with laser excitation, as described in Sec. 2.4. Although tumor tissue from injected mice consistently showed a ~fivefold greater fluorescence than the autofluorescence of noninjected controls, liver and muscle tissues, which did not express the folate receptor, displayed no difference in fluorescence intensity, regardless of the presence or absence of folate-fluorescein pretreatment (Fig. 2). Unfortunately, because of this autofluorescence, direct quantitation of folate-fluorescein uptake into malignant and nonmalignant tissues could not be determined. However, based on previous quantitative biodistribution studies of other low molecular folate conjugates,[16,22,26–28] we project that folate-fluorescein distribution *in vivo* will follow the biodistribution of folate receptors accessible to the blood, i.e., high uptake in the tumor and kidney with little or no uptake in other tissues. Furthermore, because these previous reports have shown the main route of excretion to be through the kidneys,[16,26–28] and since clearance of the fluorescein conjugate from nontargeted tissues was similarly rapid (i.e., <2 h), we assume that excretion of folate-fluorescein also occurs mainly through the kidneys.

In order to test the ability of folate-fluorescein to facilitate detection of microscopic tumor nodules, metastatic tumors of M109 cell origin were induced by inoculation of cells either into the peritoneal cavity (i.p.) or femoral vein (i.v.) of the syngeneic mice. After allowing sufficient time for tumor growth, tumor loci were again imaged by intravenous administration of folate-fluorescein followed by laser excitation. As seen in Fig. 3, metastatic tumor nodules smaller than 0.5 mm were readily observable in both lungs of the intravenously inoculated mice, and all tumor metastases fluoresced intensely compared with adjacent nonmalignant tissue. Similar results were also obtained in the intraperitoneal metastatic tumor model when the peritoneal cavity was opened and imaged as described earlier (not shown).

To further explore the ability of folate-fluorescein to image small metastatic lesions, L1210 cells were also inoculated intravenously into syngeneic mice and the various anatomical regions were again imaged as described earlier. Since L1210 cells are lymphocytic in origin and relatively small in size, they are capable of forming tumor nodules throughout the body after i.v. injection, rather than becoming entrapped primarily in the lung capillary network. As shown in Fig. 4, both upper and lower lobes of the liver contained multiple microscopic nodules that were clearly revealed under laser illumination. Furthermore, the animal's spleen was almost entirely filled with minute fluorescent tumor loci [Figs. 5(a) and 5(b)] and was consequently enlarged to roughly twice its normal size. Tumor nodules were also found in muscle tissue near the shoulder [Figs. 5(c) and 5(d)] and in the brain, spinal cord, and along the pleura (not shown). In fact, tumor nodules were seen in most tissues of the body and no nodules were identified that did not fluoresce under laser illumination.

Since methotrexate is a folate analog with two orders of magnitude lower affinity for the folate receptor than folic acid,[29] it was decided that a comparison of the uptake of folate-fluorescein, methotrexate-fluorescein, and amino fluorescein (nonbinding control) might allow a better assessment of the importance of ligand affinity on tumor-targeted optical imaging. For this purpose, equal amounts (10 nmol) of the three compounds were injected intravenously into mice with subcutaneous M109 tumors, and the tumors along with various normal tissues were compared for fluorescence intensity. As expected from their relative affinities [folate-fluorescein binds to the folate receptor with 44% the affinity of folic acid (Dr. Chris Leamon, Endocyte Inc., personal communication) and methotrexate-fluorescein displays an affinity in the micromolar range[30–32]], tumors from mice injected with folate-fluorescein fluoresced brightly, whereas tumors from mice treated with either methotrexate-fluorescein or the nontargeted amino fluorescein were not detectably more fluorescent than untreated controls (not shown). Furthermore, normal tissues from all three mice displayed only their normal autofluorescence. These results would seem to suggest that affinities in the nanomolar, but not micromolar, range are necessary to achieve good contrast between targeted and nontargeted tissues.

4 Discussion

The folate receptor is overexpressed in a number of tumors, including cancers of the ovary,[10,33,34] brain,[8,14] kidney,[11] myeloid cells,[13] lung,[10,12] and breast.[10] Using both a lung and lymphoma murine tumor model, we have shown that folate receptor-positive cancers can be optically imaged by administration of a commercially available folate-conjugated fluorescent dye. Although it was never the purpose of this study to develop the optimal probe for *in vivo* imaging, initial results with this commercially available dye suggest that characterization of tumor location, size, and growth rate by nontoxic optical methods is possible with improved fluorescent probes, optimal data collection equipment, and appropriate image reconstruction software.

Although the potential applications for folate-targeted tissue-translucent optical imaging agents seem obvious, the question naturally arises regarding the value of targeted imaging agents such as folate-fluorescein that can only reveal a malignancy when the tumor is easily exposed. We suggest two possible applications for such fluorescent probes. First, the ability of highly fluorescent conjugates to reveal a tumor's location under direct illumination might be exploited to guide

a surgeon's knife during tumor resection. For example, ovarian cancers, which are strongly folate receptor-positive, are usually asymptomatic during early stages of the disease, resulting in initial diagnoses at stage III or IV in 70% of all patients. At these late stages, there is significant spread of the cancer throughout the peritoneal cavity, with lesions commonly attached to the omentum, intestines, and other internal organs.[35] Current treatment for such advanced cancers involves debulking surgery followed by chemotherapy. It is important, to note that optimal tumor debulking has been shown to significantly increase the rate of patient survival,[36,37] suggesting that if otherwise undetected malignant masses were to be removed, a further increase in survival might be realized. We suggest that use of a folate-fluorescein or related probe in conjunction with the appropriate intraoperative viewing optics could facilitate this objective (see Fig. 4).

Second, post-treatment imaging for the recurrence of tumor nodules less than 1 cm in diameter with either computer tomography or ultrasound is often not reliable and consequently of limited value.[39] Furthermore, laparoscopy does not generally allow accurate tumor discrimination with current imaging techniques.[40] Consequently, a patient must frequently undergo a second-look surgery to determine whether a relapse has occurred. In this situation, an optical method that can distinguish cancer from noncancer tissue during an endoscopic exam could prove beneficial. With the appropriate fiber optics and the use of tumor-targeted probes such as folate-fluorescein, endoscopic evaluations of this sort might be possible. Indeed, fluorescent dyes have already been explored for their abilities to reveal tumors by fluorescent detection methods.[17,41–49] While some might raise the concern that a fluorescein probe would lose intensity during extended illumination because of photobleaching,[38] the results of this study demonstrate that photobleaching may not constitute a significant problem, at least for exposure times that are less than or equal to 1 h. Furthermore, if such problems were to arise, intermittent illumination or selection of a more photostable fluorophore could easily remedy the problem.

In summary, we have demonstrated the effectiveness of a folate-linked fluorophore for optical imaging of tumors that express the folate receptor. The difference in fluorescence intensity between folate receptor-expressing masses and nonexpressing tissues was sufficiently stark to allow the unambiguous detection of tumors that could not be identified under white light. Metastatic loci smaller than 0.5 mm in size were noticeably fluorescent compared with the background. Furthermore, uptake of the fluorophore into tissues that did not express the folate receptor was too low to cause uncertainty or misdiagnosis of the tumor, even at 2 h postinjection. These results thus raise the possibility that folate can be exploited as a targeting ligand for the visual location and resection of tumor tissue during surgery or endoscopic examination.

Acknowledgments

This work was supported by National Institutes of Health grant CA89581, Optical Therapeutic Technologies Inc., and the 21st Century Research and Technology Fund from the State of Indiana.

References

1. M. V. Knopp, E. Weiss, H. P. Sinn, J. Mattern, H. Junkermann, J. Radeleff, A. Magener, G. Brix, S. Delorme, I. Zuna, and G. van Kaick, ''Pathophysiologic basis of contrast enhancement in breast tumors,'' *J. Magn. Reson Imaging* **10**, 260–266 (1999).
2. P. J. Hudson, ''Recombinant antibodies: a novel approach to cancer diagnosis and therapy,'' *Expert Opin. Invest. Drugs* **9**, 1231–1242 (2000).
3. S. D. Jonson and M. J. Welch, ''PET imaging of breast cancer with fluorine-18 radiolabeled estrogens and progestins,'' *Q. J. Nucl. Med.* **42**, 8–17 (1998).
4. A. Heppeler, S. Froidevaux, A. N. Eberle, and H. R. Maecke, ''Receptor targeting for tumor localisation and therapy with radiopeptides,'' *Curr. Med. Chem.* **7**, 971–994 (2000).
5. J. C. Reubi, ''The role of peptides and their receptors as tumor markers,'' *Endocrinol. Metab. Clin. North Am.* **22**, 917–939 (1993).
6. J. A. Reddy and P. S. Low, ''Folate-mediated targeting of therapeutic and imaging agents to cancers,'' *Crit. Rev. Ther. Drug Carrier Syst.* **15**, 587–627 (1998).
7. X. Wang, F. Shen, J. H. Freisheim, L. E. Gentry, and M. Ratnam, ''Differential stereospecificities and affinities of folate receptor isoforms for folate compounds and antifolates,'' *Biochem. Pharmacol.* **44**, 1898–1901 (1992).
8. T. A. Patrick, D. M. Kranz, T. A. van Dyke, and E. J. Roy, ''Folate receptors as potential therapeutic targets in choroid plexus tumors of SV40 transgenic mice,'' *J. Neuro-Oncol.* **32**, 111–123 (1997).
9. G. Toffoli, C. Cernigoi, A. Russo, A. Gallo, M. Bagnoli, and M. Boiocchi, ''Overexpression of folate binding protein in ovarian cancers,'' *Int. J. Cancer* **74**, 193–198 (1997).
10. P. Garin-Chesa, I. Campbell, P. E. Saigo, J. L. Lewis, Jr., L. J. Old, and W. J. Rettig, ''Trophoblast and ovarian cancer antigen LK26. Sensitivity and specificity in immunopathology and molecular identification as a folate-binding protein,'' *Am. J. Pathol.* **142**, 557–567 (1993).
11. W. J. Rettig, C. Cordon-Cardo, J. P. Koulos, J. L. Lewis, H. F. Oettgen, and L. J. Old, ''Cell surface antigens of human trophoblast and choriocarcinoma defined by monoclonal antibodies,'' *Int. J. Cancer* **35**, 469–475 (1985).
12. W. A. Franklin, M. Waintrub, D. Edwards, K. Christensen, P. Prendegrast, J. Woods, P. A. Bunn, and J. F. Kolhouse, ''New anti-lung-cancer antibody cluster 12 reacts with human folate receptors present on adenocarcinoma,'' *Int. J. Cancer* **8**, 89–95 (1994).
13. J. F. Ross, H. Wang, F. G. Behm, P. Mathew, M. Wu, R. Booth, and M. Ratnam, ''Folate receptor type beta is a neutrophilic lineage marker and is differentially expressed in myeloid leukemia,'' *Cancer* **85**, 348–357 (1999).
14. S. D. Weitman, R. H. Lark, L. R. Coney, D. W. Fort, V. Frasca, V. R. Zurawski, Jr., and B. A. Kamen, ''Distribution of the folate receptor GP38 in normal and malignant cell lines and tissues,'' *Cancer Res.* **52**, 3396–4401 (1992).
15. S. D. Konda, M. Aref, M. Brechbiel, and E. C. Wiener, ''Development of a tumor-targeting MR contrast agent using the high-affinity folate receptor: work in progress,'' *Invest. Radiol.* **35**, 50–57 (2000).
16. S. Wang, J. Luo, D. A. Lantrip, D. J. Waters, C. J. Mathias, M. A. Green, P. L. Fuchs, and P. S. Low, ''Design and synthesis of [111In]DTPA-folate for use as a tumor-targeted radiopharmaceutical,'' *Bioconjugate Chem.* **8**, 673–679 (1997).
17. C. H. Tung, Y. Lin, W. K. Moon, and R. Weissleder, ''A receptor-targeted near-infrared fluorescence probe for in vivo tumor imaging,'' *Chembiochem.* **8**, 784–786 (2002).
18. N. P. Barry, A. Bower, S. D. Konda, A. Singha, E. C. Wiener, and E. C. Gratton, ''Near infrared contrast agent for tumor cells expressing the high affinity folate receptor,'' *Biophys. J.* **80**, 656.39 (2001).
19. D. E. Fleischer, ''Chromoendoscopy and magnification endoscopy in the colon,'' *Gastrointest Endosc* **49**, S45–S49 (1999).
20. H. Stepp, R. Sroka, and R. Baumgartner, ''Fluorescence endoscopy of gastrointestinal diseases: basic principles, techniques, and clinical experience,'' *Endoscopy* **30**, 379–386 (1998).
21. M. M. Acosta and H. W. Boyce, Jr., ''Chromoendoscopy—where is it useful?'' *J. Clin. Gastroenterol.* **27**, 13–20 (1998).
22. M. D. Kennedy, K. Jallad, J. Lu, S. Low Philip, and D. Ben-Amotz, ''Evaluation of folate conjugate uptake and transport by the choroid plexus of mice,'' *Pharm. Res.* **20**, 714–719 (2003).
23. S. Wang, R. J. Lee, C. J. Mathias, M. A. Green, and P. S. Low, ''Synthesis, purification, and tumor cell uptake of 67Ga-

deferoxamine—folate, a potential radiopharmaceutical for tumor imaging,'' *Bioconjugate Chem.* **7**, 56–62 (1996).
24. S. Achilefu, R. Dorshow, J. Bugaj, and R. Rajagopalan, ''Novel receptor-targeted fluorescent contrast agents for *in vivo* tumor imaging,'' *Invest. Radiol.* **35**, 479–485 (2000).
25. A. Becker, C. Hessenius, K. Licha, B. Ebert, U. Sukowski, W. Semmler, B. Wiedenmann, and C. Grotzinger, ''Receptor-targeted optical imaging of tumors with near-infrared fluorescent ligands,'' *Nat. Biotechnol.* **19**, 327–331 (2001).
26. C. J. Mathias, S. Wang, D. J. Waters, J. J. Turek, P. S. Low, and M. A. Green, ''Indium-111-DTPA-folate as a potential folate-receptor-targeted radiopharmaceutical,'' *J. Nucl. Med.* **39**, 1579–1585 (1998).
27. C. J. Mathias, S. Wang, P. S. Low, D. J. Waters, and M. A. Green, ''Receptor-mediated targeting of 67Ga-deferoxamine-folate to folate-receptor-positive human KB tumor xenografts,'' *Nucl. Med. Biol.* **26**, 23–25 (1999).
28. C. J. Mathias, D. Hubers, P. S. Low, and M. A. Green, ''Synthesis of [(99m)Tc]DTPA-folate and its evaluation as a folate-receptor-targeted radiopharmaceutical,'' *Bioconjugate Chem.* **11**, 253–257 (2000).
29. M. Ratnam and J. H. Freisheim, *Folic Acid Metabolism in Health and Disease*, pp. 91–120, Wiley Liss, New York (1990).
30. T. P. McAlinden, J. B. Hynes, S. A. Patil, G. R. Westerhof, G. Jansen, J. H. Schornagel, S. S. Kerwar, and J. H. Freisheim, ''Synthesis and biological evaluation of a fluorescent analogue of folic acid,'' *Biochemistry* **30**, 5674–5681 (1991).
31. G. R. Gapski, J. M. Whiteley, J. I. Rader, P. L. Cramer, G. B. Henderson, V. Neef, and F. M. Huennekens, ''Synthesis of a fluorescent derivative of amethopterin,'' *J. Med. Chem.* **18**, 526–528 (1975).
32. G. B. Henderson, A. Russell, and J. M. Whiteley, ''A fluorescent derivative of methotrexate as an intracellular marker for dihydrofolate reductase in L1210 cells,'' *Arch. Biochem. Biophys.* **202**, 29–34 (1980).
33. I. G. Campbell, T. A. Jones, W. D. Foulkes, and J. Trowsdale, ''Folate-binding protein is a marker for ovarian cancer,'' *Cancer Res.* **51**, 5329–5338 (1991).
34. J. F. Ross, P. K. Chaudhuri, and M. Ratnam, ''Differential regulation of folate receptor isoforms in normal and malignant tissues *in vivo* and in established cell lines. Physiologic and clinical implications,'' *Cancer* **73**, 2432–2443 (1994).
35. M. Boente, A. Godwin, and W. Hogan, ''Screening, imaging and early diagnosis of ovarian cancer,'' *Clin. Obstet. Gynecol.* **37**, 377–391 (1994).
36. A. R. Munkarah, A. V. Hallum, M. Morris, T. W. Burke, C. Levenback, E. N. Atkinson, J. T. Wharton, and D. M. Gershenson, ''Prognostic significance of residual disease in patients with stage IV epithelial ovarian cancer,'' *Gynecol. Oncol.* **64**, 13–17 (1997).
37. J. P. Curtin, R. Malik, E. S. Venkatraman, R. R. Barakat, and W. J. Hoskins, ''Stage IV ovarian cancer: impact of surgical debulking,'' *Gynecol. Oncol.* **64**, 9–12 (1997).
38. L. Song, E. J. Hennink, I. T. Young, and H. J. Tanke, ''Photobleaching kinetics of fluorescein in quantitative fluorescence microscopy,'' *Biophys. J.* **68**, 2588–2600 (1995).
39. C. Murolo, S. Costantini, G. Foglia, T. Guido, F. Odicino, M. Pace, S. Parodi, G. Pino, N. Ragni, and L. Repetto, ''Ultrasound examination in ovarian cancer patients. A comparison with second look laparotomy,'' *J. Ultrasound Med.* **8**, 441–443 (1989).
40. M. Piver, S. Lele, J. Barlow et al., ''Second-look laparoscopy prior to proposed second-look parotomy,'' *Obstet. Gynecol. (N.Y., NY, U. S.)* **55**, 571 (1980).
41. B. Ballou, G. W. Fisher, A. S. Waggoner, D. L. Farkas, J. M. Reiland, R. Jaffe, R. B. Mujumdar, S. R. Mujumdar, and T. R. Hakala, ''Tumor labeling *in vivo* using cyanine-conjugated monoclonal antibodies,'' *Cancer Immunol. Immunother* **41**, 257–263 (1995).
42. B. Ballou, G. W. Fisher, T. R. Hakala, and D. L. Farkas, ''Tumor detection and visualization using cyanine fluorochrome-labeled antibodies,'' *Biotechnol. Prog.* **13**, 649–658 (1997).
43. K. Licha, C. Hessenius, A. Becker, P. Henklein, M. Bauer, S. Wisniewski, B. Wiedenmann, and W. Semmler, ''Synthesis, characterization, and biological properties of cyanine-labeled somatostatin analogues as receptor-targeted fluorescent probes,'' *Bioconjugate Chem.* **12**, 44–50 (2001).
44. S. Folli, G. Wagnieres, A. Pelegrin, J. M. Calmes, D. Braichotte, F. Buchegger, Y. Chalandon, N. Hardman, C. Heusser, and J. C. Givel, ''Immunophotodiagnosis of colon carcinomas in patients injected with fluoresceinated chimeric antibodies against carcinoembryonic antigen,'' *Proc. Natl. Acad. Sci. U.S.A.* **89**, 7973–7977 (1992).
45. S. Folli, P. Westermann, D. Braichotte, A. Pelegrin, G. Wagnieres, H. van den Bergh, and J. P. Mach, ''Antibody-indocyanin conjugates for immunophotodetection of human squamous cell carcinoma in nude mice,'' *Cancer Res.* **54**, 2643–2649 (1994).
46. R. Hornung, A. L. Major, M. McHale, L. H. L. Liaw, L. A. Sabiniano, B. J. Tromberg, M. W. Berns, and Y. Tadir, ''*In vivo* detection of metastatic ovarian cancer by means of 5-aminolevulinic acid-induced fluorescence in a rat model,'' *J. Am. Assoc. Gynecol. Laparosc* **5**, 141–148 (1998).
47. M. M. Haglund, M. S. Berger, and D. W. Hochman, ''Enhanced optical imaging of human gliomas and tumor margins,'' *Neurosurgery* **38**, 308–317 (1996).
48. B. Ballou, G. W. Fisher, J. S. Deng, T. R. Hakala, M. Srivastava, and D. L. Farkas, ''Cyanine fluorochrome-labeled antibodies *in vivo*: assessment of tumor imaging using Cy3, Cy5, Cy5.5, and Cy7,'' *Cancer Detect. Prev.* **22**, 251–257 (1998).
49. C. H. Tung, S. Bredow, U. Mahmood, and R. Weissleder, ''Preparation of a cathepsin D sensitive near-infrared fluorescence probe for imaging,'' *Bioconjugate Chem.* **10**, 892–896 (1999).